

Electronic Supplementary Information

The role of the dihedral angle and excited cation states in ionization and dissociation of mono-halogenated biphenyls; a combined experimental and theoretical coupled cluster study

Michael Barclay¹, Ragnar Bjornsson^{*2,3}, Maicol Cipriani², Andreas Terfort⁴, Howard Fairbrother¹, Oddur Ingólfsson^{*2}

Address:

¹Department of Chemistry, Johns Hopkins University, Baltimore, Maryland 21218, USA

²Department of Chemistry and Science Institute, University of Iceland, Dunhagi 3, 107 Reykjavik, Iceland

³Current address: Department of Inorganic Spectroscopy, Max-Planck-Institut für Chemische Energiekonversion, Stiftstrasse 34-36, 45470 Mülheim an der Ruhr (Germany).

⁴Department of Chemistry, Institute of Inorganic and Analytical Chemistry, Goethe-University, 60438 Frankfurt, Germany

Email: O. Ingólfsson - odduring@hi.is, R. Bjornsson - ragnar.bjornsson@gmail.com

* Corresponding authors

Comparison of our DLPNO-CCSD(T) calculated ionization energies with accurate experimental data

Table S1. Experimental and calculated adiabatic ionization energies (eV) of halobenzenes. Calculations are DLPNO-CCSD(T)/CBS (def2-SVP/def2-TZVP extrapolation) on B3LYP-D3/def2-TZVP geometries including ZPE calculated with B3LYP-D3/def2-TZVP. Note that the thermal energy of the neutral molecule is not included here as the experimental IEs correspond to 0 K values.

Molecule	Exp. IE ^a	Calc. IE
C ₆ H ₅ F	9.2032 ± 0.0006 ^a	9.204
C ₆ H ₆	9.24378 ± 0.00007 ^b	9.197
C ₆ H ₅ Cl	9.0728 ± 0.0006 ^a	9.107
C ₆ H ₅ Br	8.9975 ± 0.0006 ^a	9.045
C ₆ H ₅ I	8.7580 ± 0.0006 ^a	8.837

^a From one-photon mass-analyzed threshold ionization spectrometry by Kwon, C. H.; Kim, H. L.; Kim, M. S. *J. Chem. Phys.* **2002**, *116*, 10361-10371.

^b Average of two ZEKE measurements: 9.24384 ± 0.00006 and 9.24372 ± 0.00005 by Nemeth, G.I.; Selzle, H.L.; Schlag, E.W., *Chem. Phys. Lett.*, **1993**, *215*, 151 and Chewter, L.A.; Sander, M.; Muller-Dethlefs, K.; Schalg, E.W., *J. Chem. Phys.*, **1987**, *86*, 4737.

Basis set convergence study of halogen threshold energies of halobenzenes

Table S2 below demonstrates the accuracy that can be achieved in our DLPNO-CCSD(T) calculations when basis set convergence is pushed to the limit including accounting for core-correlation effects.

Table S2. DLPNO-CCSD(T) calculated thresholds (eV) of C₆H₅X where X=Cl, Br and I with different basis sets. Atomic spin-orbit coupling corrections were added to the halogen atom threshold energies: 0.036, 0.152 and 0.314 eV for Cl, Br and I, respectively. Also included are zero-point vibrational energy (at the B3LYP-D3/def2-TZVP level of theory) contributions for the reaction (-0.163, -0.147 and -0.136 eV for C₆H₅Cl, C₆H₅Br and C₆H₅I reactions respectively). A frozen core was used unless specified.

Molecule	Exp. ^a	cc-pwCV5Z-PP no frozen core. ^b	cc-pwCV5Z-PP frozen core. ^b	cc-pV5Z _b	cc-pVQZ-PP ^b	cc-pVTZ-PP ^b	cc-pVDZ-PP ^b	def2-SVP/def2-TZVP extrapolation
C ₆ H ₅ Cl	12.454±0.04	12.449	12.418	12.409	12.332	12.179	11.894	12.384
C ₆ H ₅ Br	11.810±0.05	11.798	11.789	11.829	11.791	11.620	11.327	11.836
C ₆ H ₅ I	11.140±0.07	11.153	11.142	11.199	11.138	10.970	10.647	11.192

^a Derived experimental values from Stevens, W.; Sztaray, B.; Shuman, N.; Baer, T.; Troe, J. *J. Phys. Chem. A*, **2009**, *113*, 573-582.

^b Tight pair natural orbital (PNO) thresholds were used.

Calculated barriers

Table S3. Calculated barriers in eV (relative to the parent neutral molecule) for HX formation from 2-Cl-BPh, 2-I-BPh and 2-I-BPh ground-state cations.

Molecule	Same-ring HX Barrier	Diff-ring HX Barrier 1	Diff-ring HX Barrier 2
2-Cl-BPh	12.14	12.54	12.58
2-Br-BPh	11.83	11.23	12.50
2-I-BPh	11.43	10.93	12.09

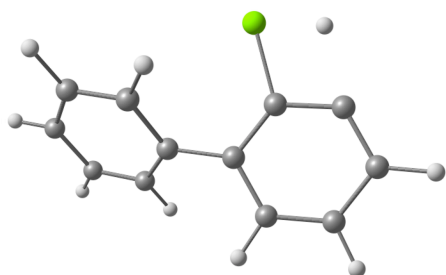


Figure S2. Saddlepoint geometry for 2-Cl-BPh for same-ring HX formation.

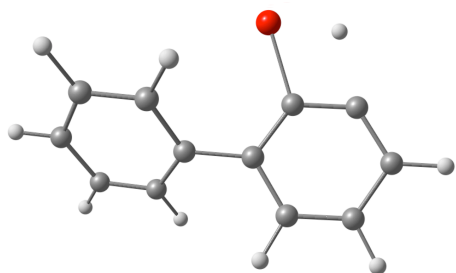


Figure S3. Saddlepoint geometry for 2-Br-BPh for same-ring HX formation.

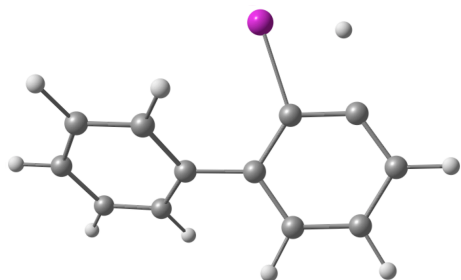


Figure S4. Saddlepoint geometry for 2-I-BPh for same-ring HX formation.

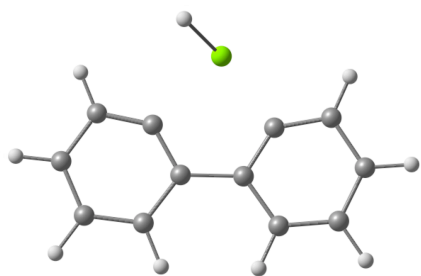


Figure S5. Saddlepoint geometry no. 1 for 2-Cl-BPh for diff-ring HX formation

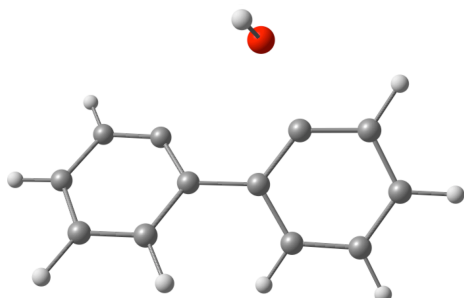


Figure S6. Saddlepoint geometry no. 1 for 2-Br-BPh for diff-ring HX formation

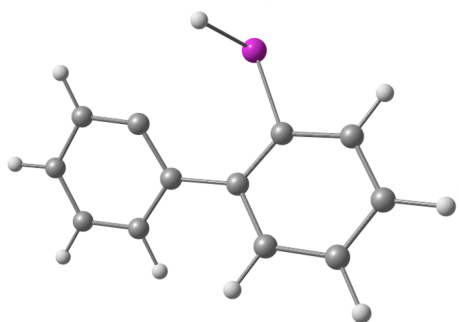


Figure S7. Saddlepoint geometry no. 1 for 2-I-BPh for diff-ring HX formation

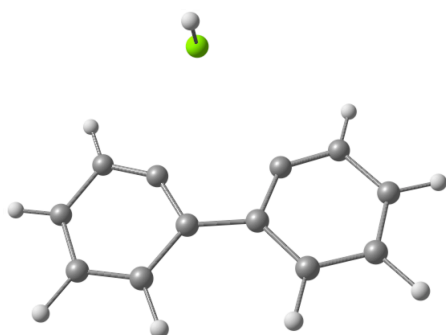


Figure S8. Saddlepoint geometry no. 2 for 2-Cl-BPh for diff-ring HX formation

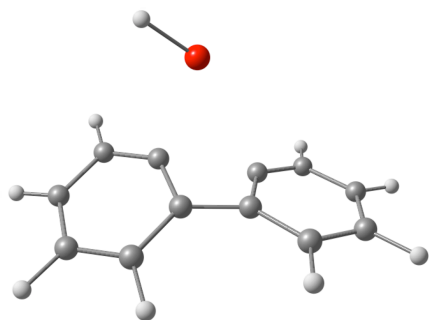


Figure S9. Saddlepoint geometry no. 2 for 2-Br-BPh for diff-ring HX formation

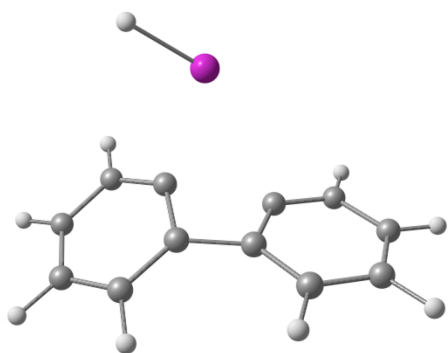


Figure S10. Saddlepoint geometry no. 2 for 2-I-BPh for diff-ring HX formation

Cartesian coordinates (Å) of the DFT-optimized structures in this study

See compressed zip archive (ESI-Barclay-xyzfiles.zip) containing XYZ files of all molecules and fragments.